Lunar Imaging and Ionospheric Calibration for the Lunar Cherenkov Technique

Dr Rebecca McFadden[1,2]

O. Scholten[2] M. Mevius[2] S. Buitink[2] J. Bray[3] R. Ekers[3]

1 ASTRON Netherlands Institute for Radio Astronomy, The Netherlands
2 Rijksuniversiteit Groningen 3 CSIRO Astronomy and Space Science, Australia

Image by Emil Lenc[3]

UHE Neutrino Detection using the Lunar Cherenkov Technique

neutrino

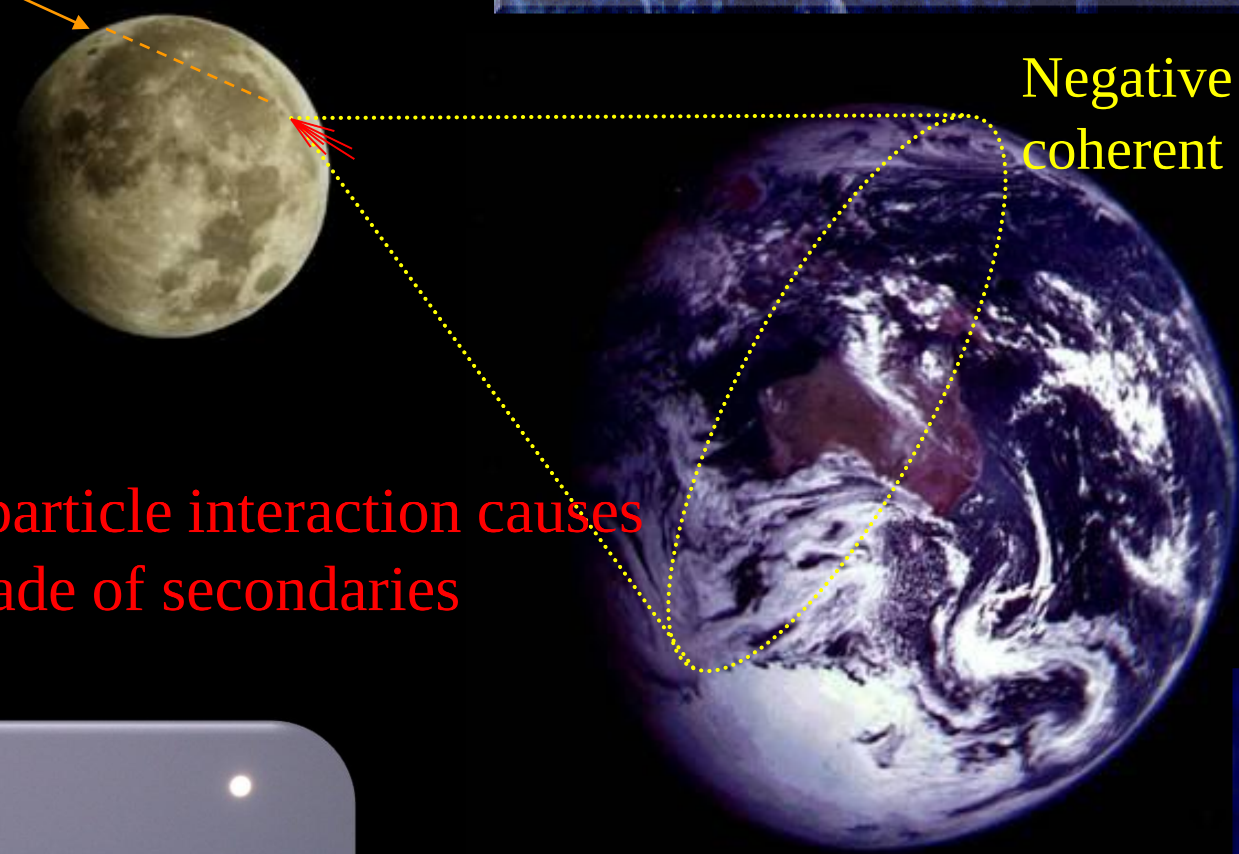

Negative charge excess produces coherent Cherenkov radiation

UHE particle interaction causes a cascade of secondaries

Technique first proposed by Dagkesamanskii & Zhelezynkh (1989) and first applied by Hankins, Ekers and O'Sullivan (1996) using the Parkes radio telescope

Characteristics of Radio Emission

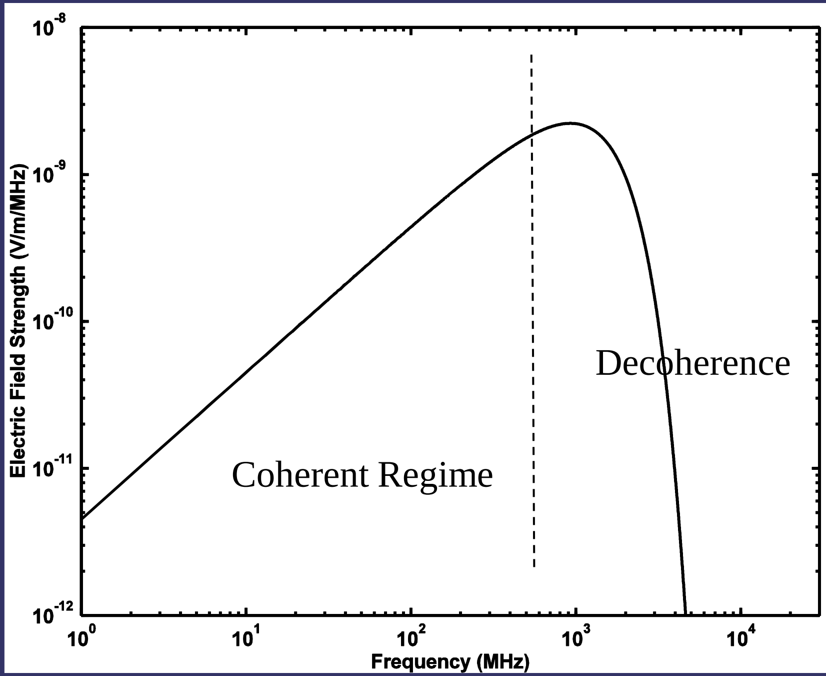

Spectrum

- Broadband continuous emission
- Coherent emission process
- Peak depends on viewing angle (< 5GHz)

Pulse Profile

- Very narrow unmodulated pulse (ns scale)
- Broad receiver bandwidth for ns time resolution
- High speed sampling
- Real time trigger to avoid excessive storage requirements

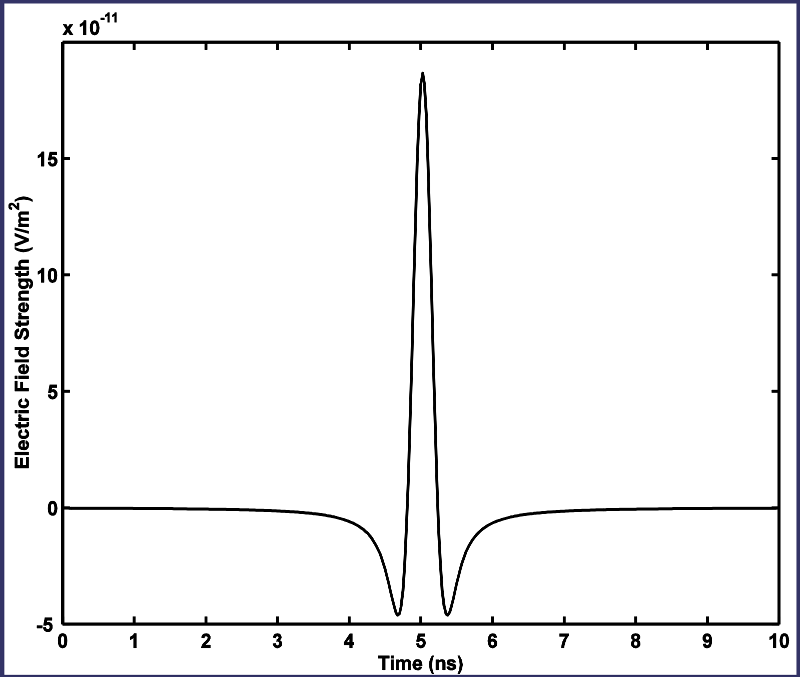

Ionospheric Dispersion

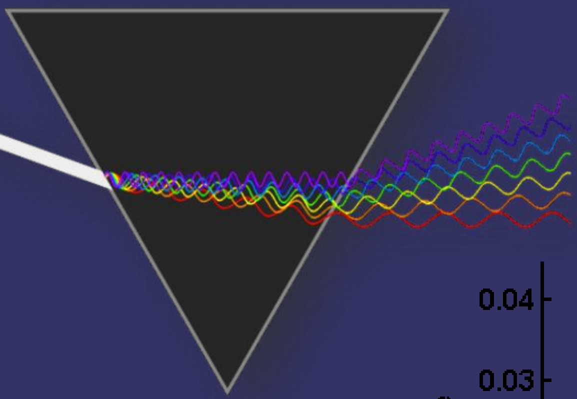

- Ionospheric dispersion destroys the characteristic coherency of the pulses.
- The effect is worse at low frequencies and for high ionospheric TEC (related to diurnal cycle, solar cycle and latitude of observation).

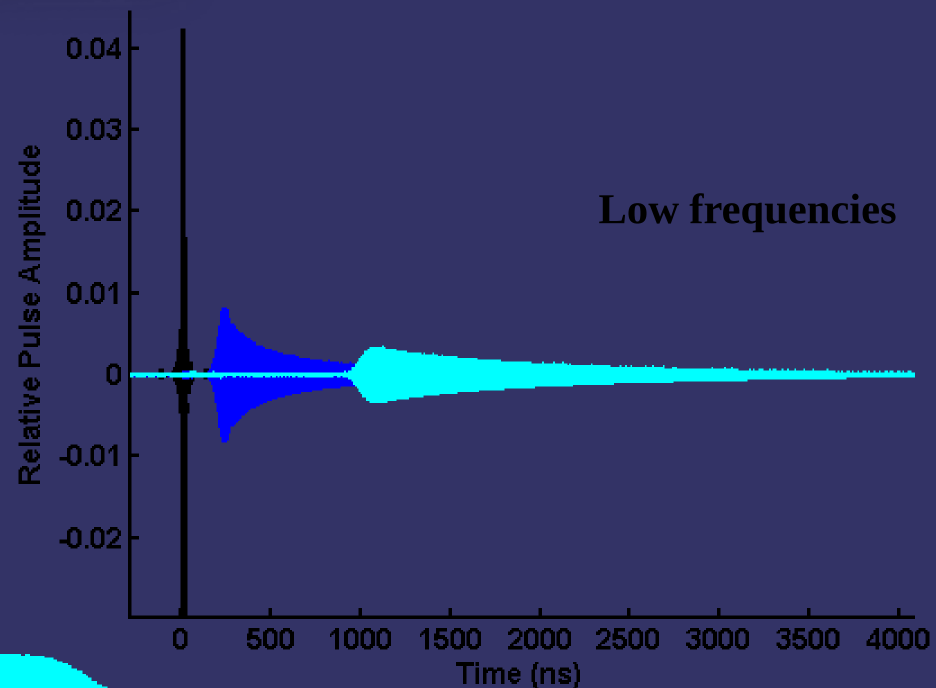

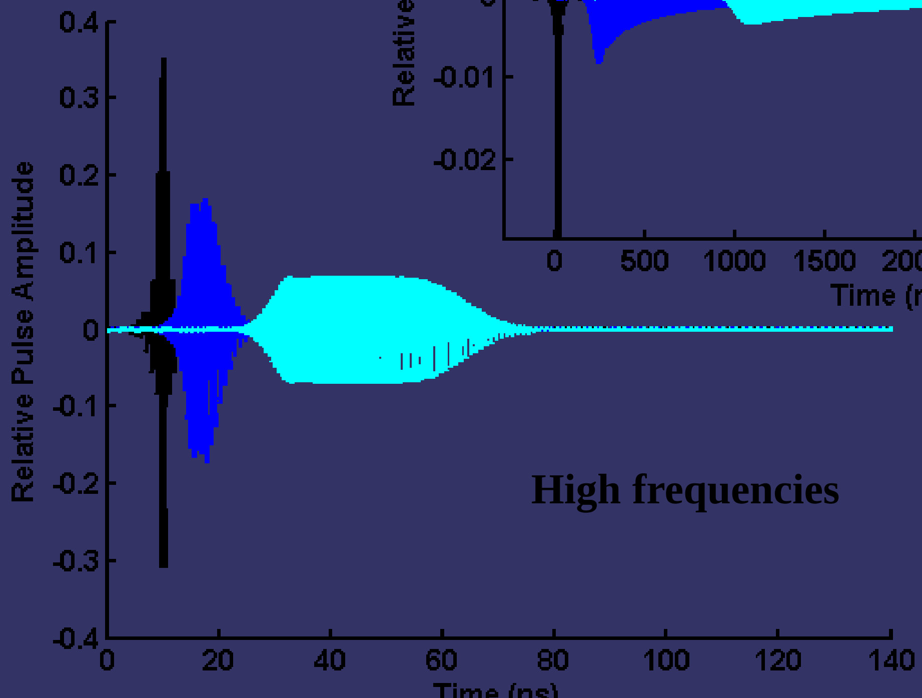

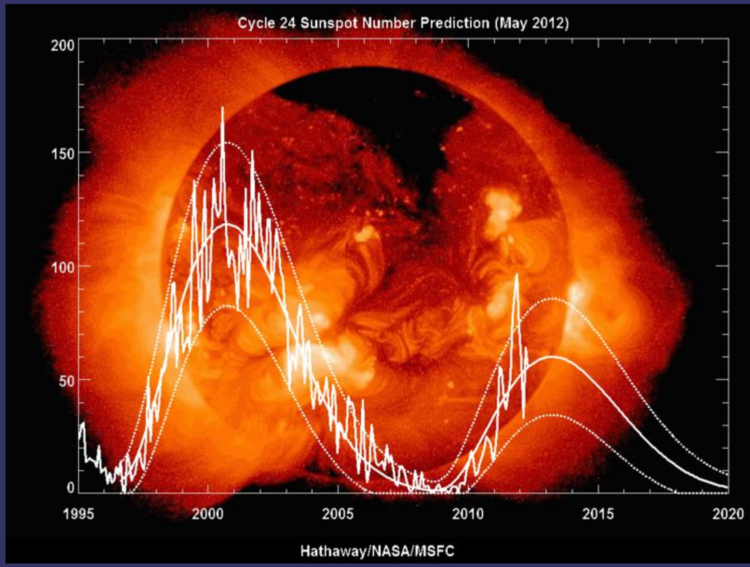

Ionospheric Products

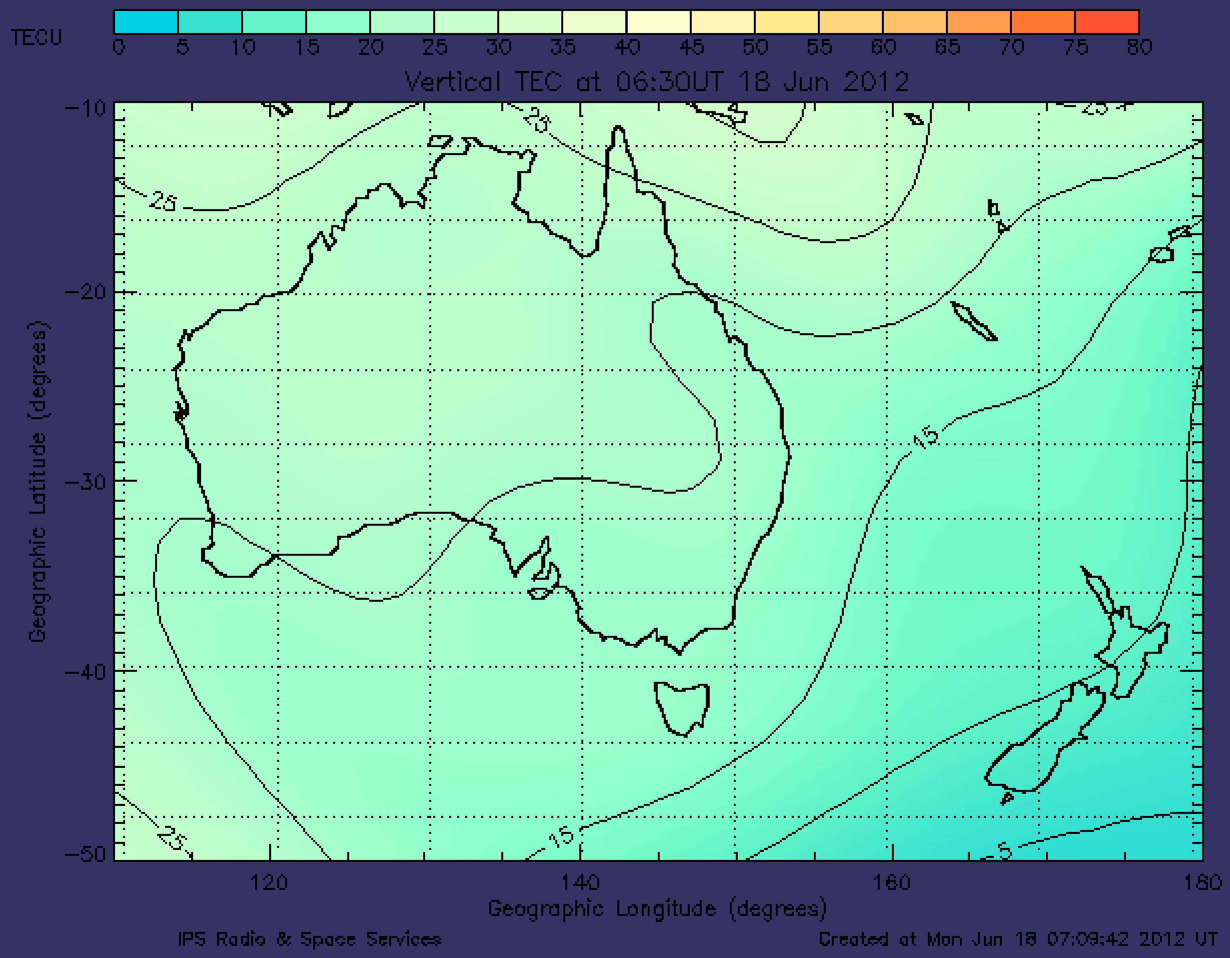

Australian Ionospheric Prediction Service

Available in 15 min intervals

Based on GPS data

Includes FoF2 ionosonde data

Two layer modelling
- SLM ionosphere
- Plasmaspheric modelling

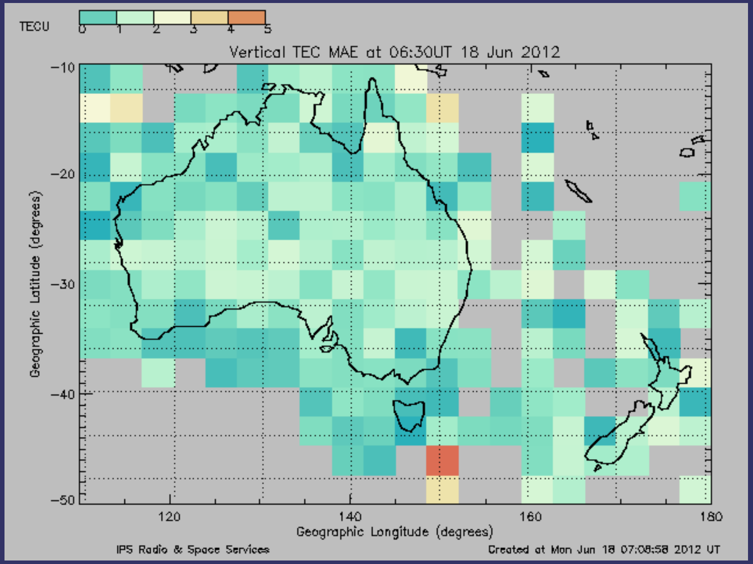

An Alternative Method for Atmospheric Dispersion Calibration

Proposed at the Merida ICRC 2007 (McFadden et. al.) and initially developed for the LUNASKA (see #240) Collaboration using the Australia Telescope Compact Array.

Ionospheric TEC can be deduced from Faraday rotation measurements of a polarised source combined with geomagnetic field models.

We propose to use this technique, with the polarised thermal radio emission from the lunar limb as our polarised source, to obtain **instantaneous** and **line-of-sight** TEC measurements.

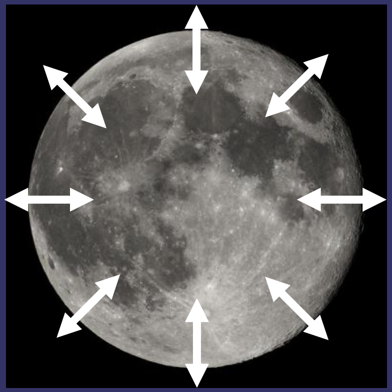

Lunar polarisation distribution – radially aligned

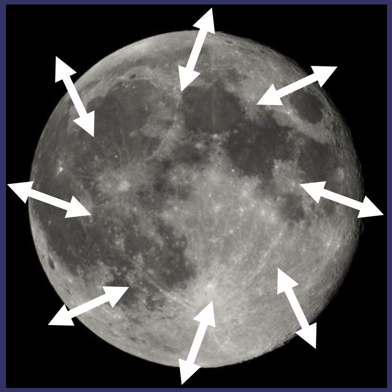

Faraday rotation from the ionosphere

Lunar Polarisation Distribution

First described by Heiles and Drake (1963)

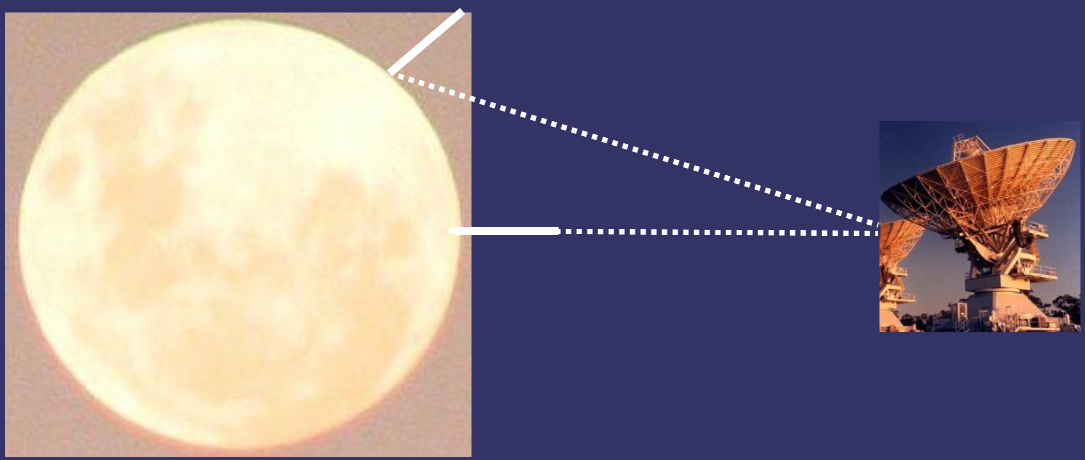

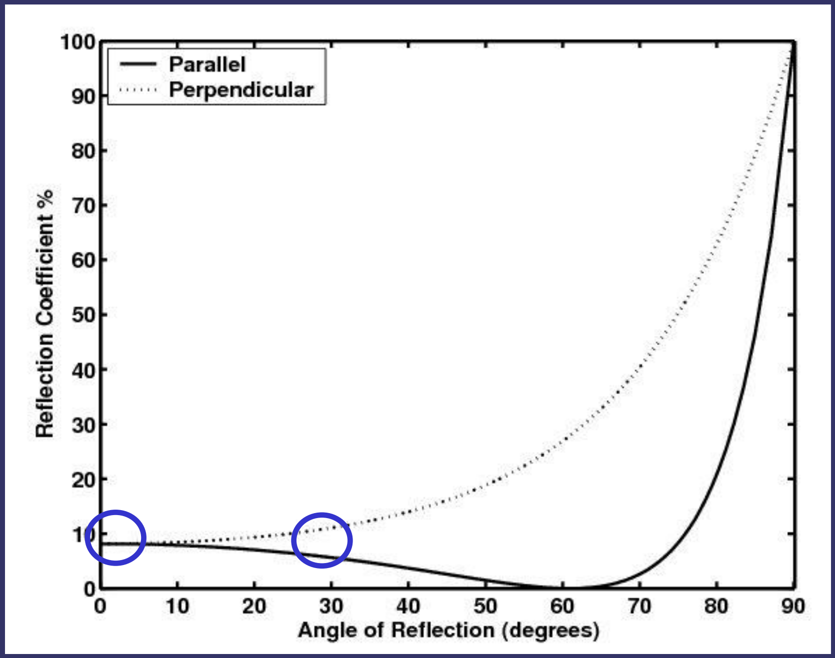

Lunar (planetary) polarisation distribution is due to Brewster angle effects and the changing viewing angle (with respect to the planetary surface normal).

Visibility domain PA Distribution

Position Angle Distributions

$$PA = \frac{1}{2}\tan^{-1}(U/Q)$$

U **Q**

Lunar Distribution

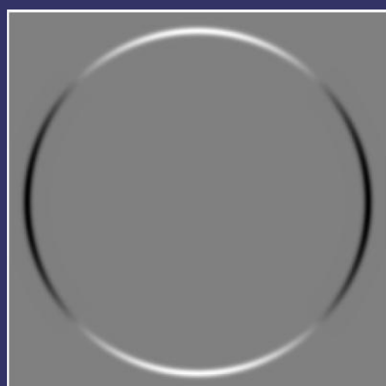

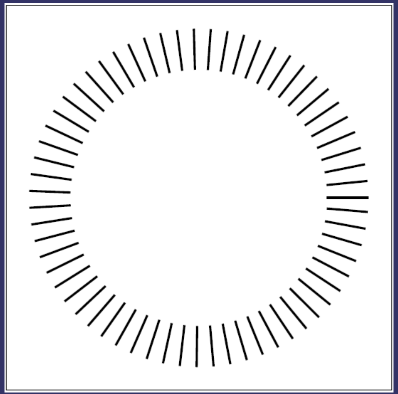

uv plane distribution

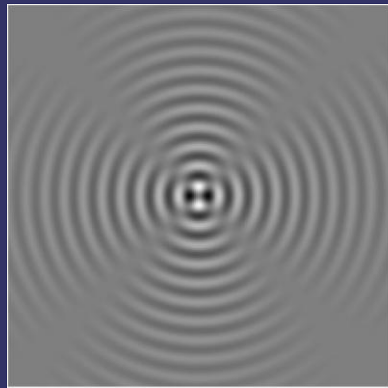

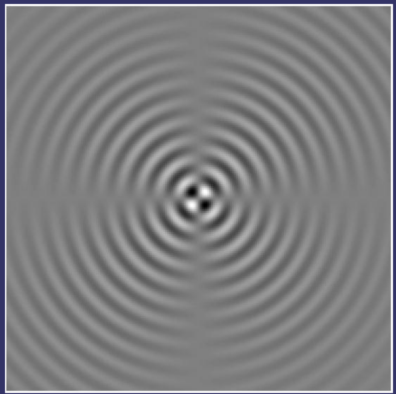

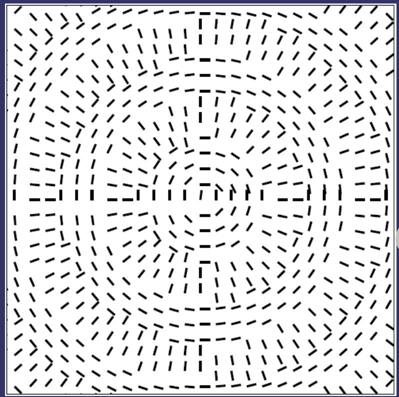

not to scale
(zoomed in to show structure)

Data generated in Matlab - to model images in the visibility domain

PA Measurements in the visibility domain

For and East-West array, baseline projection traces an ellipse through the uv plane

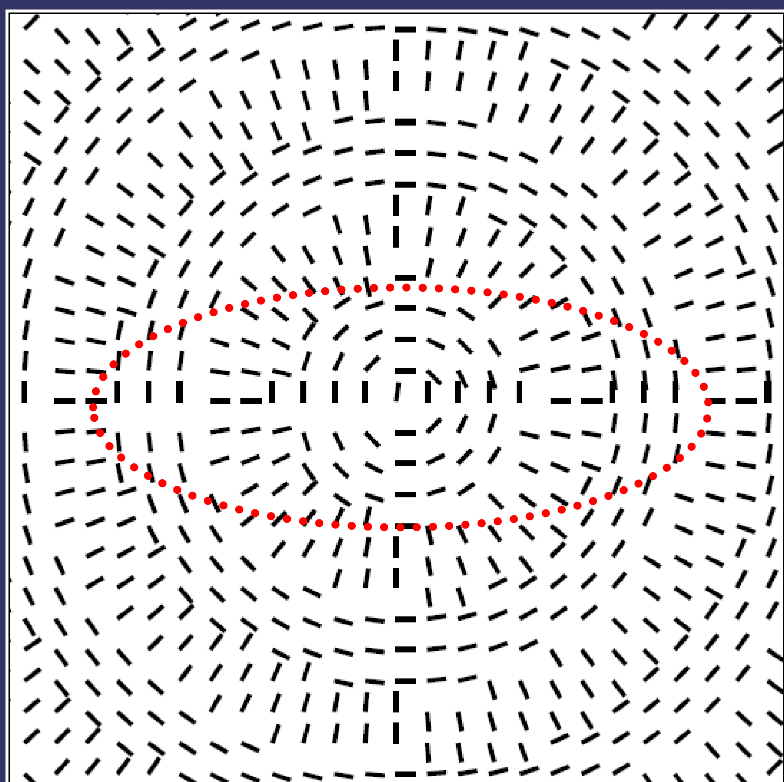

Position Angle map

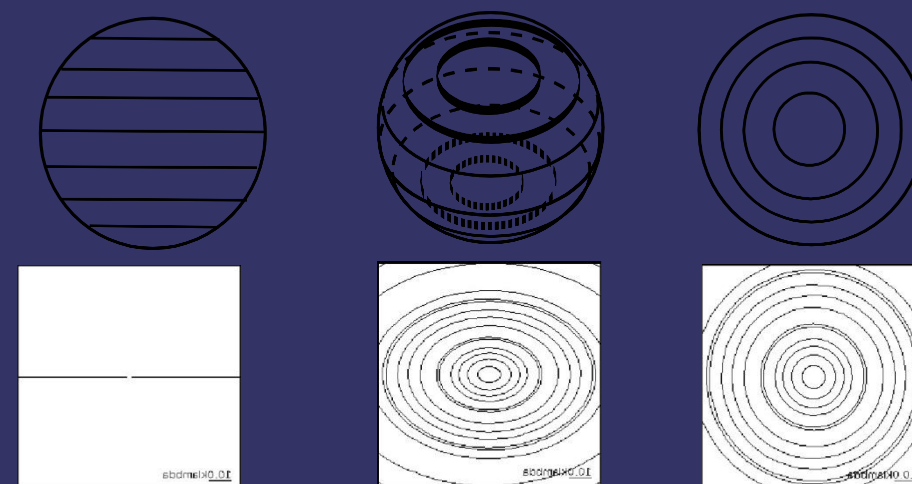

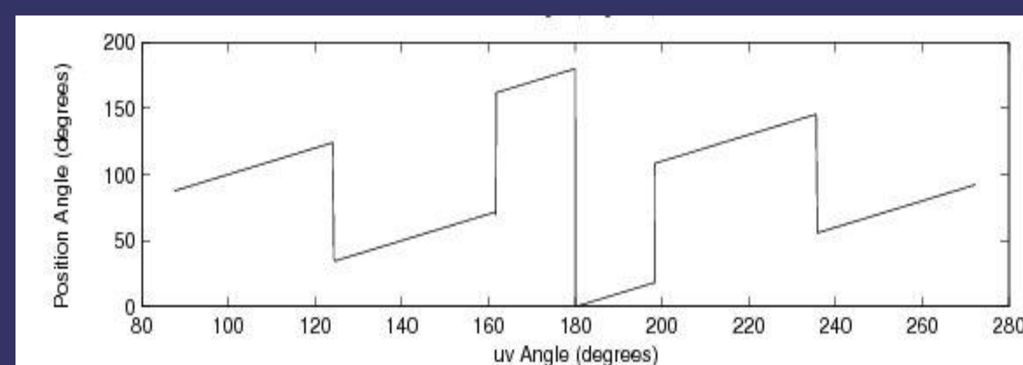

UV plane Position Angle measurements from Modelled data

PA Measurements in the visibility domain

Baseline projection traces an ellipse through the uv plane

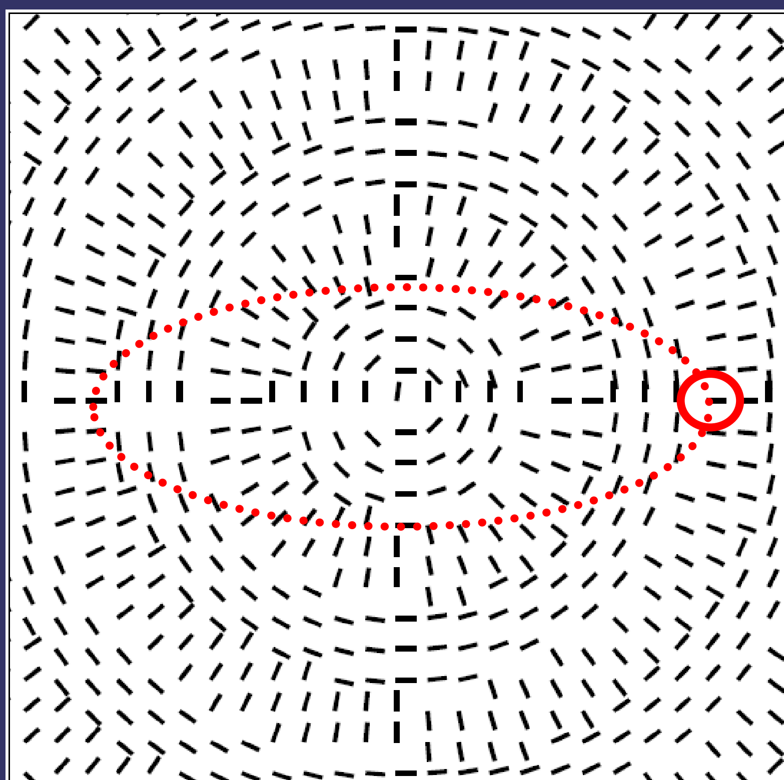

Position Angle map generated in Matlab

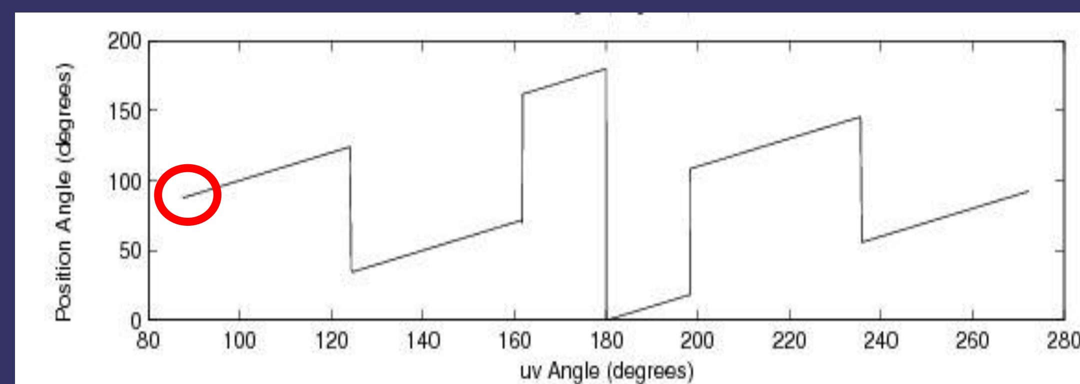

UV plane Position Angle measurements from data modelled in Miriad

PA Measurements in the visibility domain

Baseline projection traces an ellipse through the uv plane

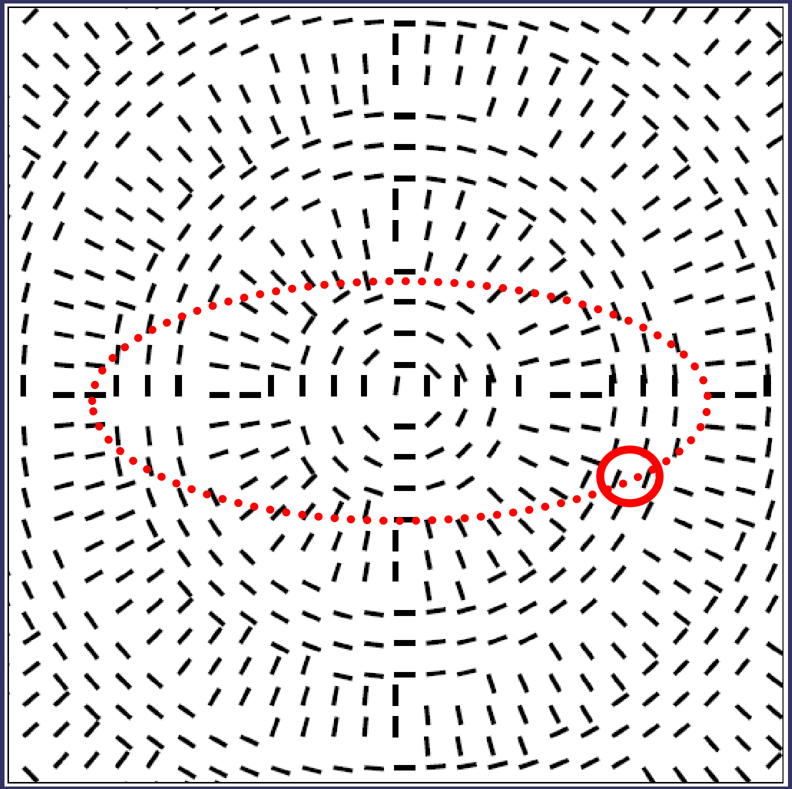

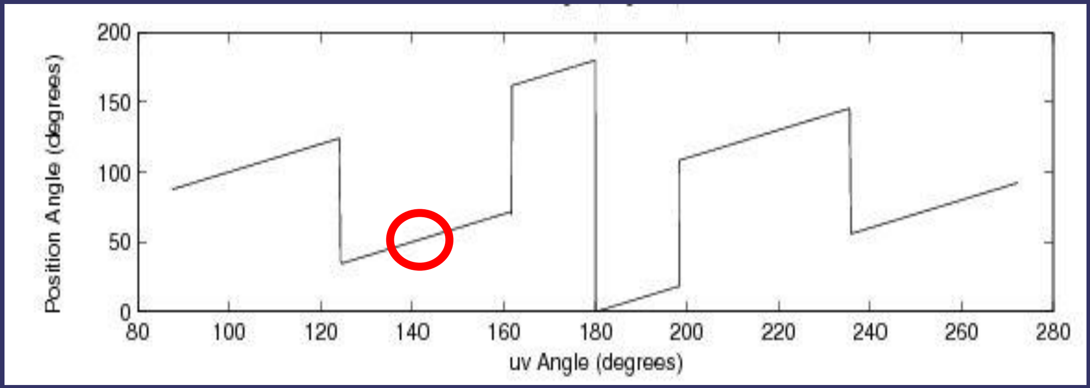

UV plane Position Angle measurements from data modelled in Miriad

Position Angle map generated in Matlab

Position Angle Measurements

Simulation

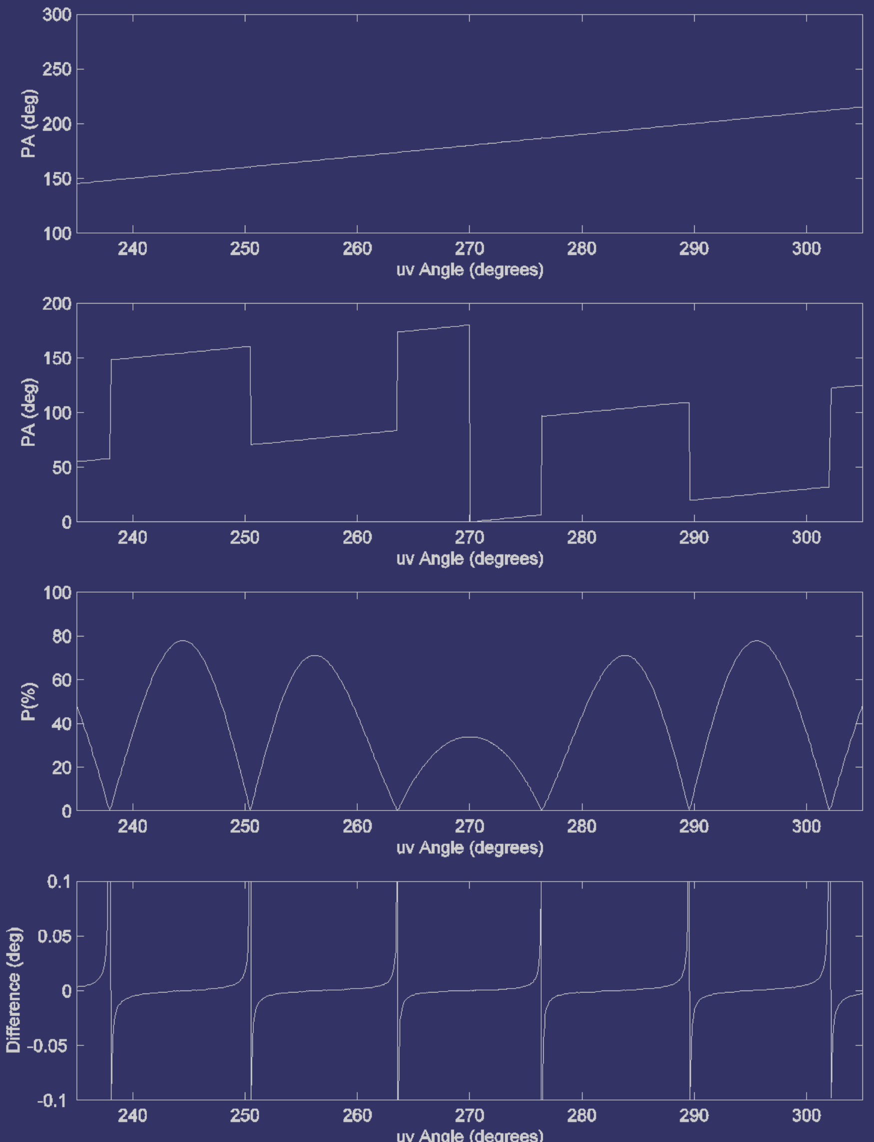

Data generated in MIRIAD using *uvgen* and imported into Matlab for analysis (no Faraday rotation)

Real Data

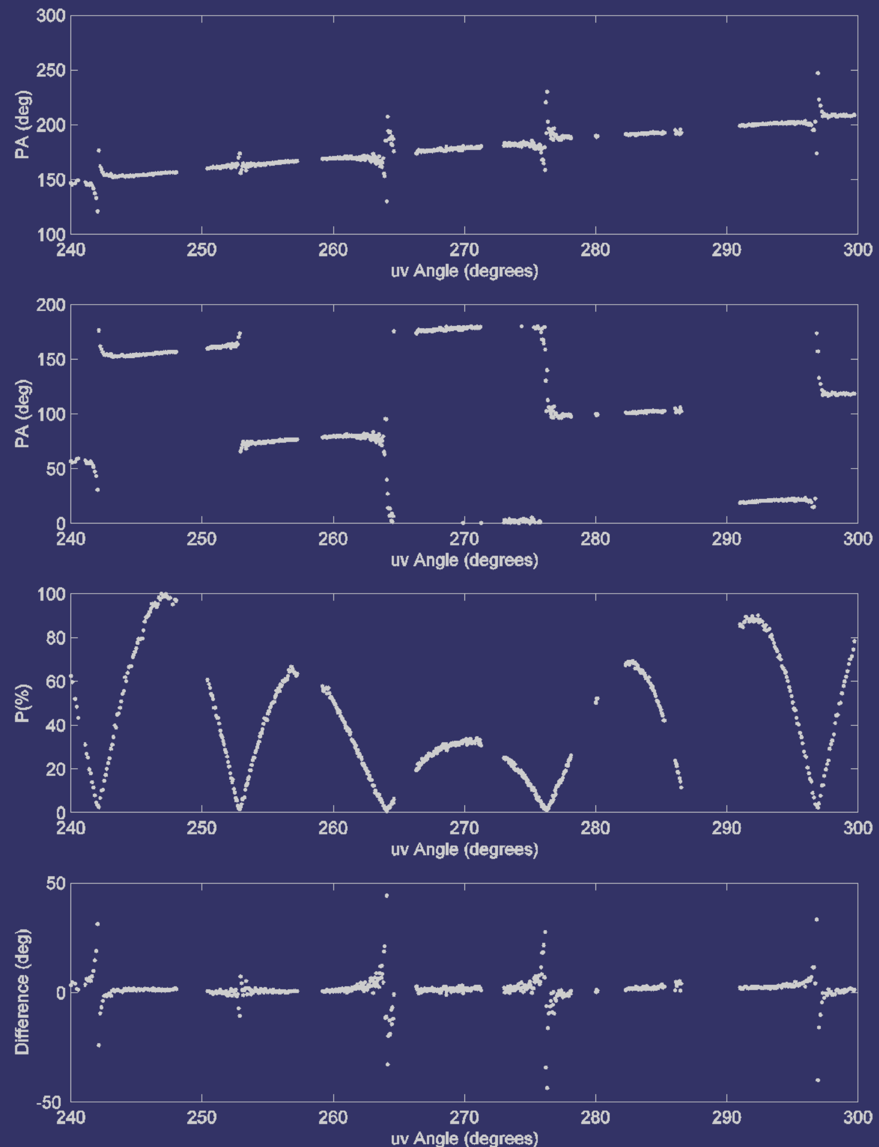

Real data taken on the ATCA, Sep 2008

GPS Comparison (TEC)

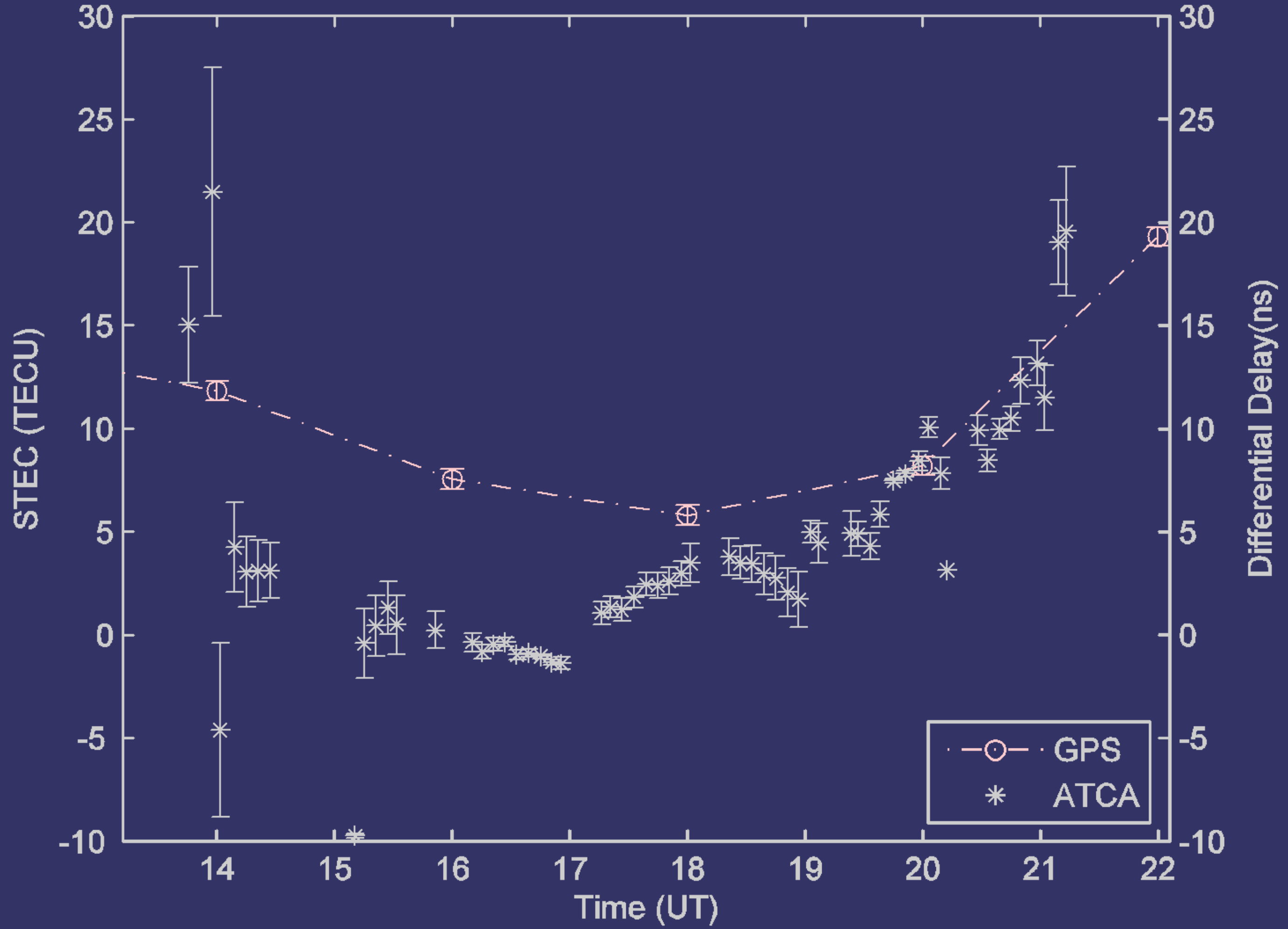

Lunar Profile Fitting

Surface roughness on a scale > 1 λ will affect emissivity.

The observed polarisation is related to the *effective* dielectric constant which is a mix of the true dielectric constant and surface roughness effects.

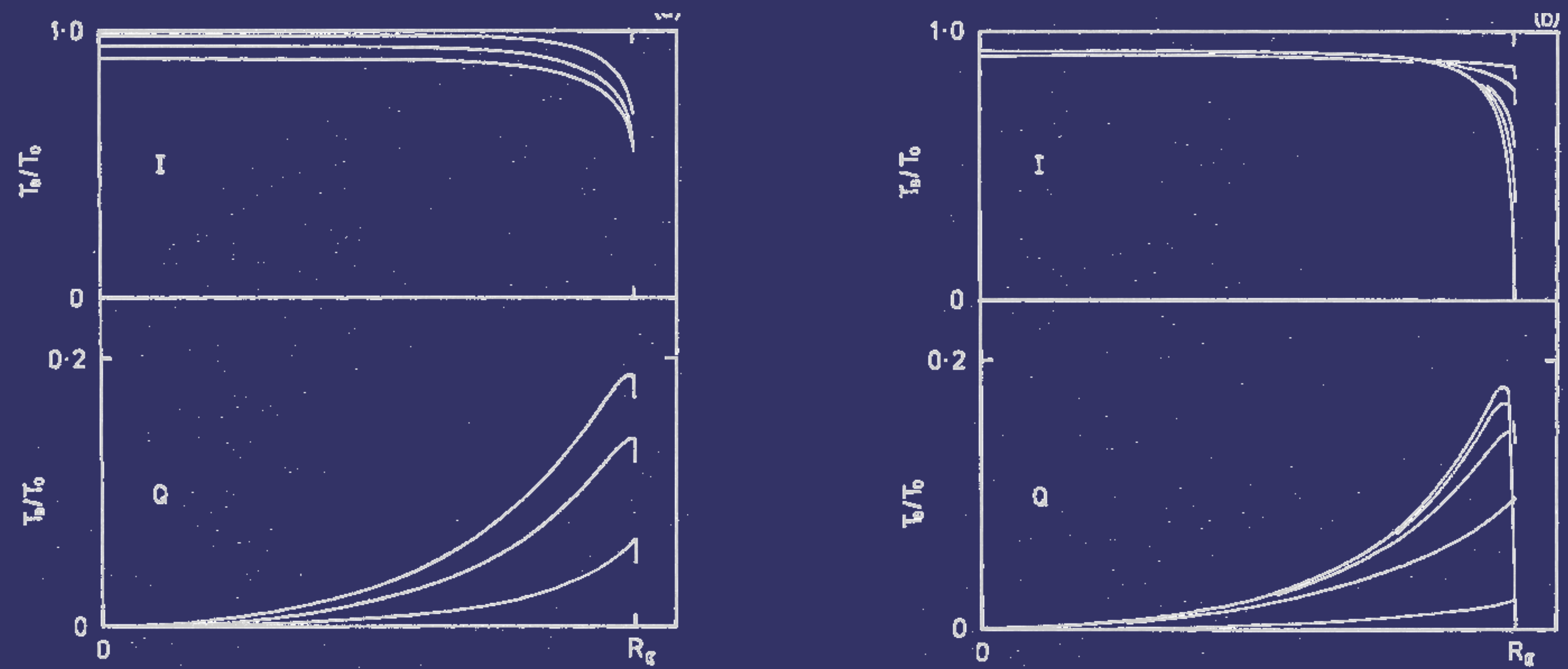

Moffat 1972 a) $\varepsilon = 1.5, 2.5, 3.5$ b) $\sigma = 5, 10, 20, 40^\circ$

see also Heiles and Drake (1963) for lunar visibility function fitting

Lunar Imaging

May be able to attribute temperature variations and polarisation defects to lunar surface features (ie Mare vs highland regions).

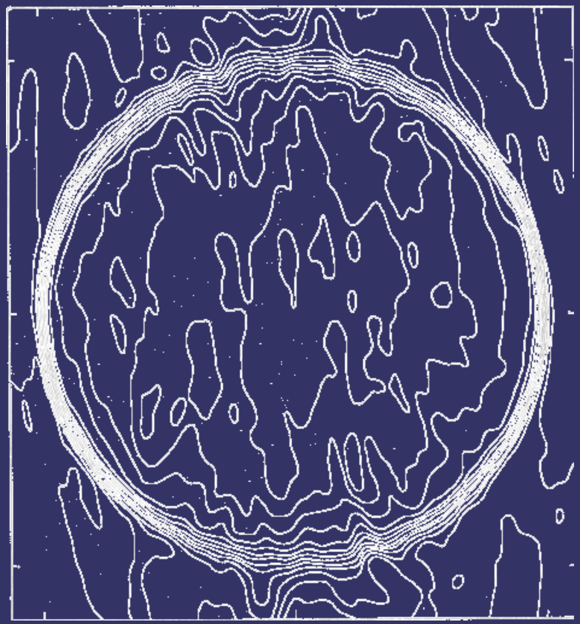

Intensity image

Moffat 1972, 1.4GHz, 10K contours

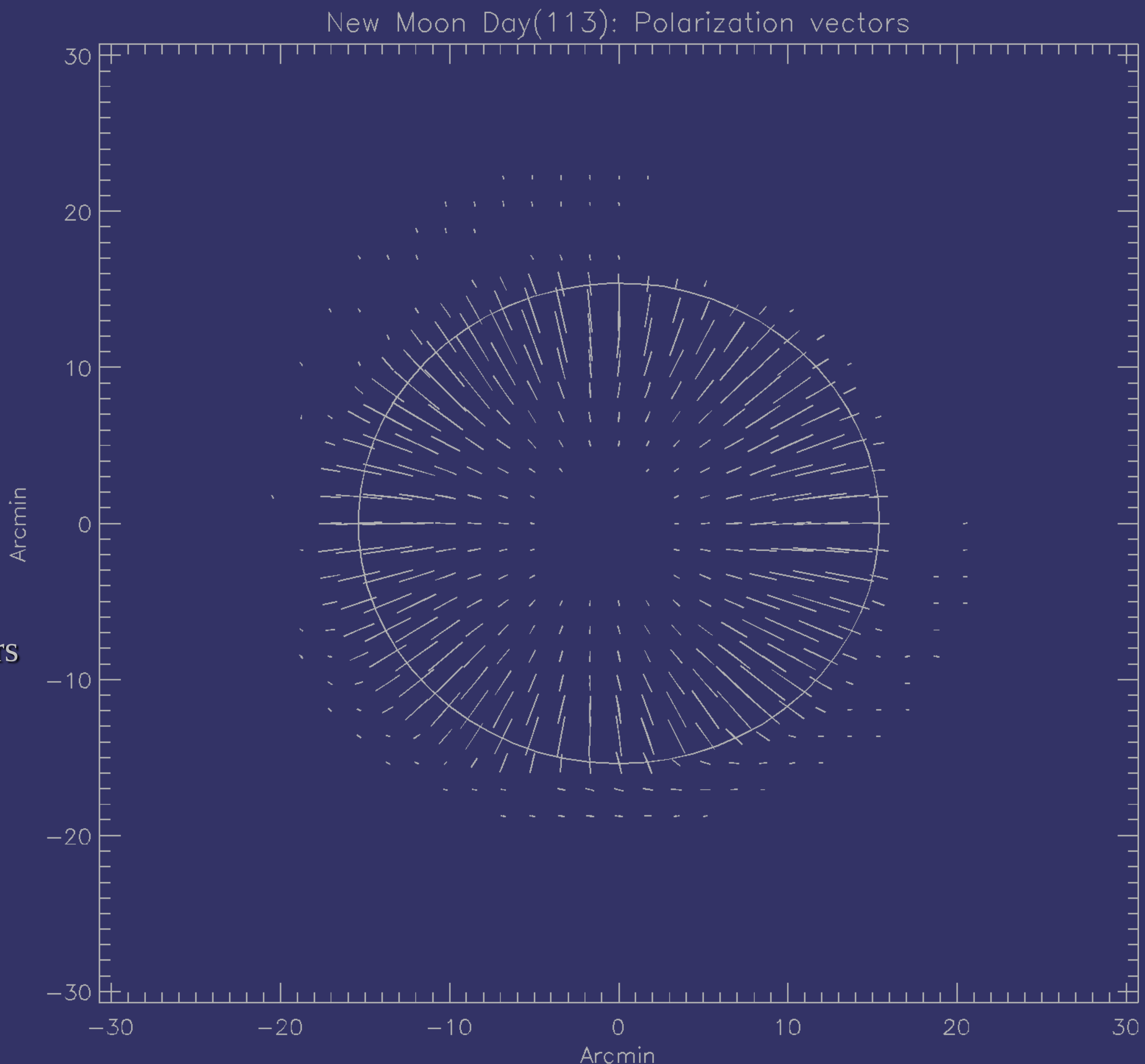

Polarisation image

SPORT collaboration 2002
8.3GHz

The Elusive Low Frequency Moon…

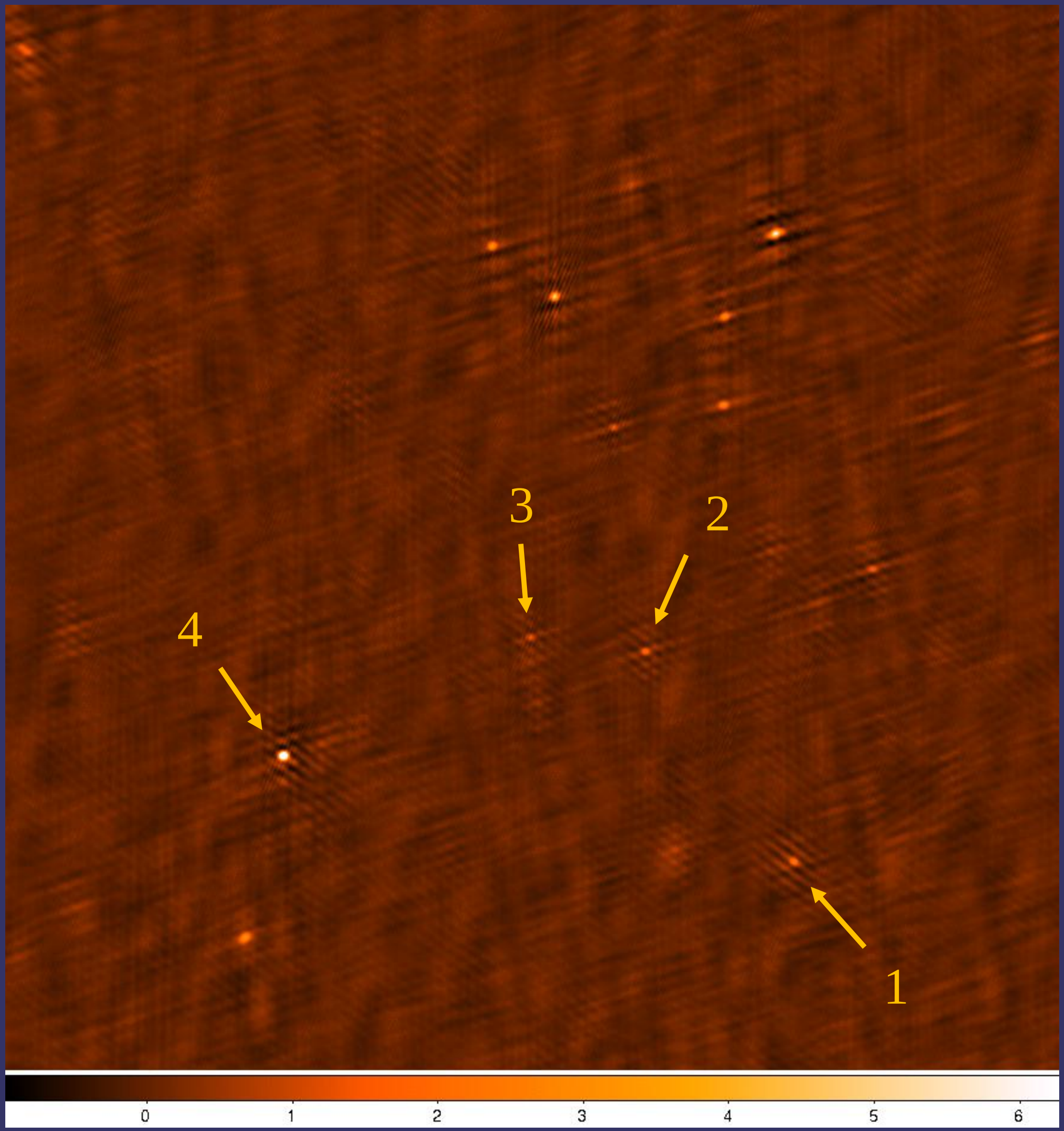

Lunar Imaging Considerations

Sky temperature is dominated by galactic radiation

$T_{sky} = T_{s0}\lambda^{2.55}$

where T_{s0} 60 ± 20K for galactic latitudes between 10 & 90 deg

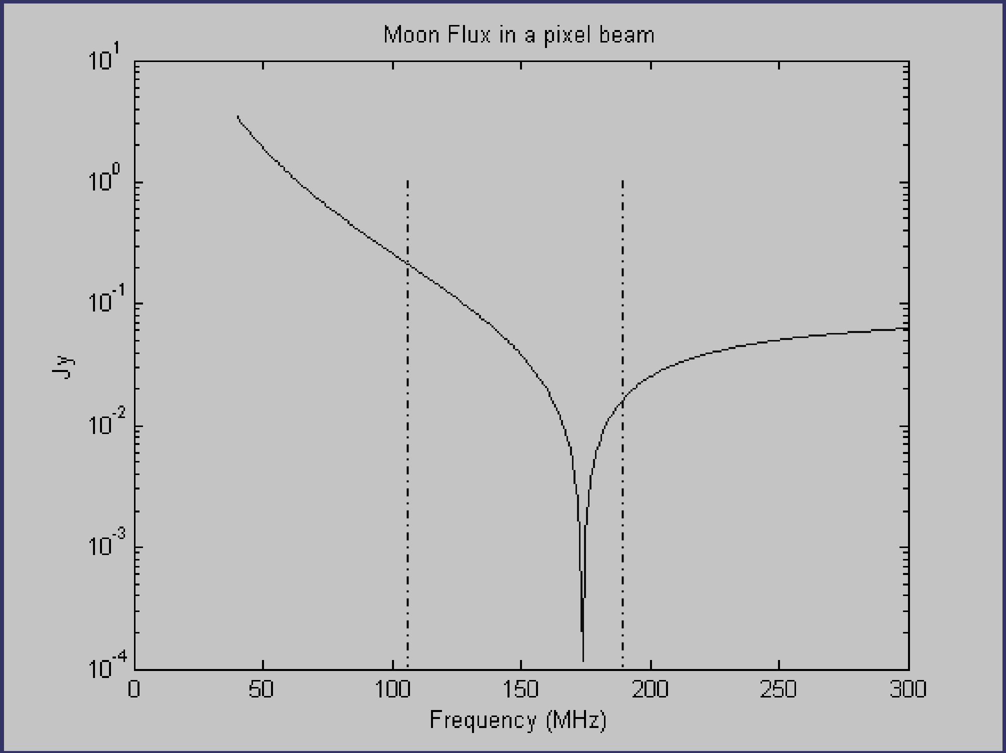

-.2 Jy @ ~100 MHz, x10 above theoretical noise level

150 MHz 100 MHz 50 MHz

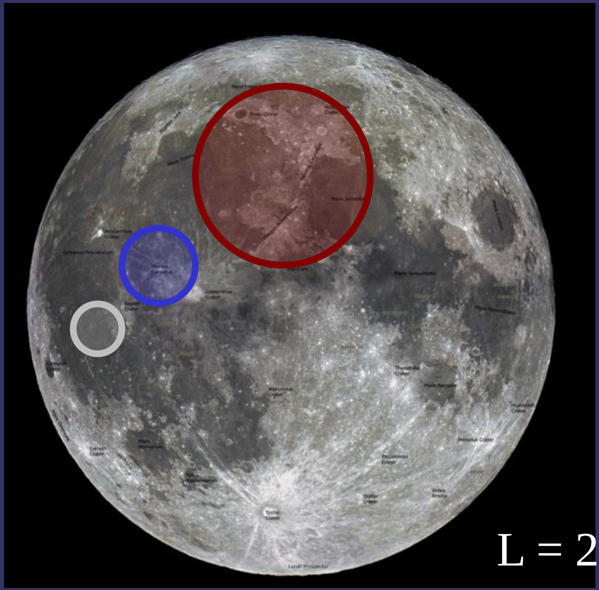

Imaging the Lunar Polarisation Distirbution

- 27 beams around limb
- beam stacking gain
- polarisation loss
- Faraday rotation estimates can be fit across th frequency band
- difficult to characterise polarised background emission due to phase screening effect

Future Work

- Calibration and imaging at 100MHz continues
- Extend to polarisation imaging and estimate Faraday rotation
- Repeat visibility domain studies with Westerbork data (1.4GHz)
- Polarisation analysis to determine and map lunar surface properties at low frequencies

Future Work

- Calibration and imaging at 100MHz continues
- Extend to polarisation imaging and estimate Faraday rotation
- Repeat visibility domain studies with Westerbork data (1.4GHz)
- Polarisation analysis to determine and map lunar surface properties at low frequencies

James 15 months

Lunar UHE Neutrino Astrophysics with the Square Kilometre Array (LUNASKA)

Work conducted by the Lunatic team will form a pathway for UHE neutrino detection using the proposed SKA radio telescope.

The Square Kilometre Array will be 100 times more sensitive than the best present day radio instruments.

The current designs proposed for the SKA consist of large numbers (~10^4) small dishes (6-12m) to achieve a square kilometre of collecting area in the 0.1-3GHz range.

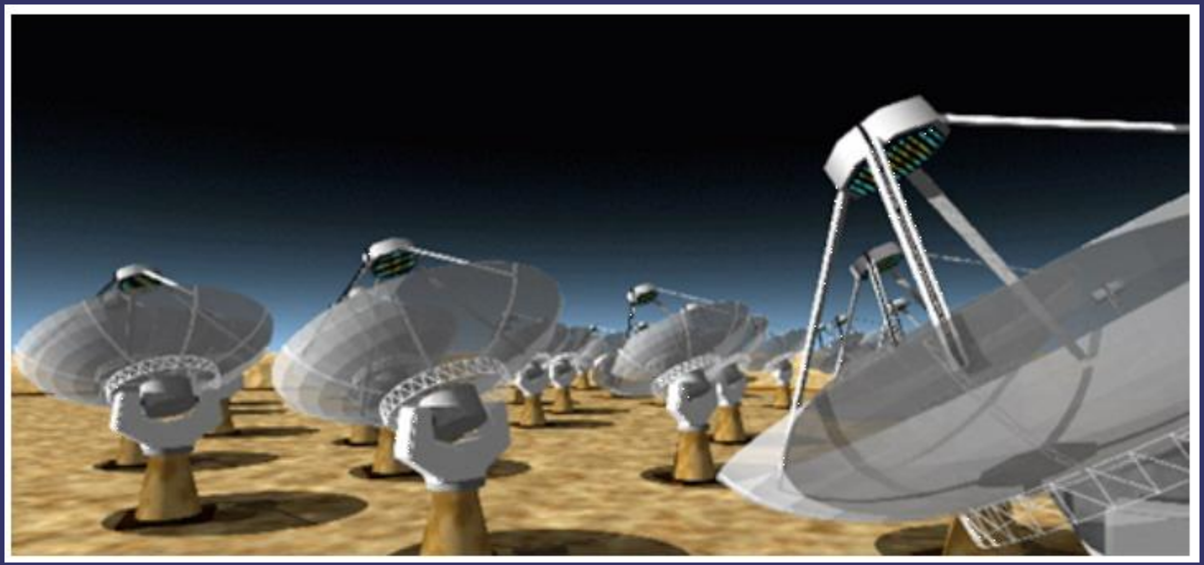

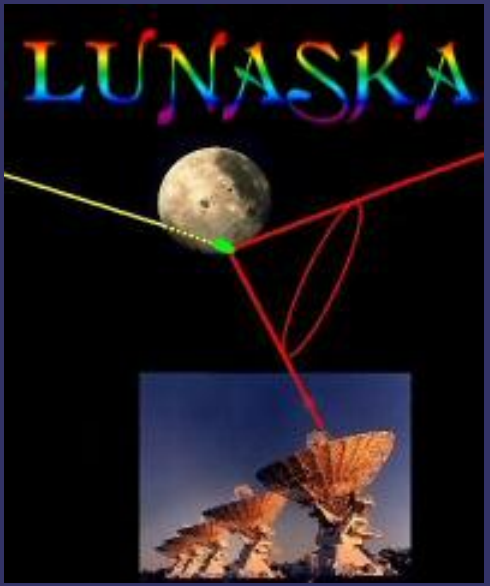

UHE Neutrinos (~10^{20} eV)

- Cosmic Ray energy spectrum extends from below 10^{10} eV to at least 10^{20} GeV

- In the rest frame of an UHECR proton, the CMB are blue shifted to gamma ray energies and the threshold for Bethe-Heitler pair production and pion photoproduction is reached.

- The origin of UHECR above this threshold (GZK cut-off) is not fully understood.

- For extragalactic UHECR almost all spectral information above the GZK cut-off is lost however significant information is preserved in the spectrum of neutrinos.

- UHE neutrino astronomy will be able to provide more insight into the origin of UHECR.

Neutrino-induced Showers

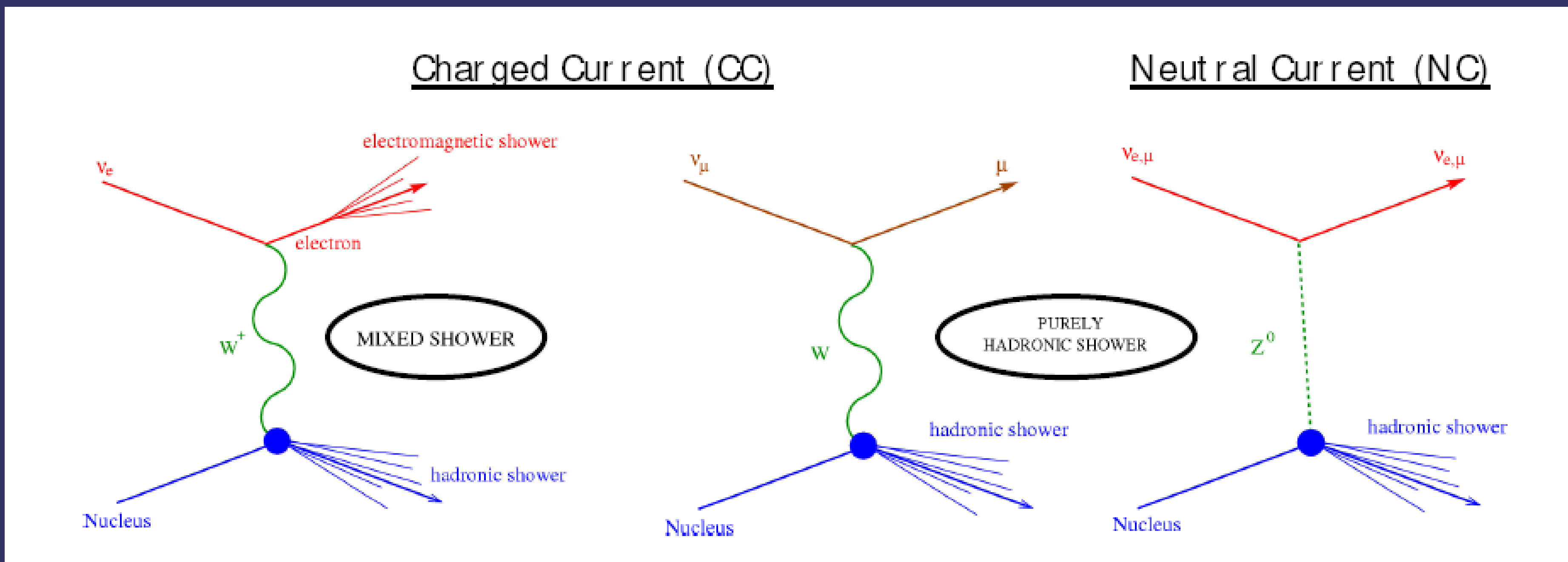

Deep inelastic scattering neutrino interactions

$E\ (\text{hadronic shower}) = y\, E_\nu$

$E\ (\text{electromagnetic shower}) = (1 - y)\, E_\nu$

inelasticity = $y \sim 0.2$ @ 10^{18} eV